Comparison of susceptibility gradient mapping and off-resonance excitation for quantitative positive contrast MRI of magnetotactic bacteria

S. Josan[1,2], A. Hamilton[3], M. Benoit[3], C. Cunningham[4], D. Spielman[2], A. Matin[3], and D. Mayer[1,2]
[1]SRI International, Menlo Park, CA, United States, [2]Radiology, Stanford University, Stanford, CA, United States, [3]Microbiology and Immunology, Stanford University, Stanford, CA, United States, [4]Sunnybrook Health Sciences Center, Toronto, ON, Canada

Introduction

Contrast agents incorporating superparamagnetic iron-oxide (SPIO) nanoparticles have shown great promise in visualizing labeled cells using MRI. The objective of this work is to explore techniques for improvements in MRI of cancer using genetically encoded magnetite as a contrast agent. The magnetotactic bacteria *Magnetospirillum magneticum* AMB-1 endogenously produce magnetite particles, and have been shown to generate positive MRI contrast in mouse xenograft tumors using T1-weighted MRI [1]. However, as the T2 shortening effect of the magnetite on the signal intensity surpasses the T1 effect, the enhanced contrast peaks within a certain range of magnetite concentration, preventing quantitative assessment. Several techniques exist for visualization of the magnetite particles, but accurate quantitation remains challenging. In this work, two positive contrast imaging techniques were implemented on a 7T small-animal scanner and evaluated for quantitative detection of the magnetite particles.

The off-resonance excitation method [2] takes advantage of the local resonance frequency shift caused by the iron particles, by using a pair of spectral-spatial RF pulses to excite and refocus only the off-resonant water protons in the vicinity of the particles while suppressing the on-resonant signal. Compared to the non-slice selective pulses used in [2], restricting the excitation to a thin slice using spectral-spatial pulses allows the ability to exclude regions with severe B_0 inhomogeneities, achieve better shim over the slice and reduces the degree of background suppression required.

The susceptibility gradient mapping (SGM) technique [3] involves post-processing of conventional 3D gradient echo (GRE) T2* weighted complex images to calculate susceptibility gradients induced by the magnetite particles. The susceptibility gradients around the particles result in a shift in k-space, which is proportional to the strength of the susceptibility gradient and is detected by a local Fourier transform of the image subsets in each of the 3 spatial dimensions. A map of the susceptibility gradient vector then provides a positive contrast image of the particle distribution.

Methods

All measurements were performed on a GE 7T small-animal MR scanner (770 mT/m, 7700 mT/m/ms) using a quadrature transmit/receive RF coil (dia=5 cm, length=7 cm). For the off-resonance imaging method a pair of spectral-spatial RF pulses were designed for a 90º excitation (B1max=0.1 G, duration=6.28 ms) and refocusing (B1max= 0.19 G, duration=5.44 ms). The imaging parameters for the phantom experiments were FOV=64 mm, 2 mm slice, TE=18 ms, TR=600 ms, 0.25 mm in-plane resolution, and 2 averages for off-resonant acquisitions. Images were acquired at on-resonance and at +350 Hz off-resonance.

The SGM method used 3D GRE complex images acquired in the axial plane with TE=10 ms, TR = 75 ms, flip angle=30º, FOV= 40x40x10 mm^3, matrix size = 160x160x40 for 0.25 mm isotropic resolution. The post-processing was implemented in Matlab as described in [3], and used a 1D Fourier transform and a quadratic polynomial fit to determine the echo shift for each voxel.

The phantom contained four 10 μL spots of AMB-1 bacterial cells in 4% gelatin, with Fe concentrations of approximately 10, 25, 50 and 75 μg/ml. The AMB-1 bacteria were grown in Magnetospirillum growth medium supplemented with Wolfe's mineral solution and ATCC vitamin supplement for bacteriological culture media 6 days, then subcultured into fresh media supplemented with 40 μM ferric malate for an additional 6 days of growth. Bacterial cell density was determined by optical density measurements and correlated to a standard curve. All harvested bacteria were washed twice in iron free media prior to phantom assembly.

Results and Discussion

Figure 1 shows a GRE image as well as positive contrast images of the phantom. Both the off-resonance excitation and the SGM post-processing techniques visualize the magnetite spots well, with good background suppression. Figure 1d shows that a linear correlation exists between the iron concentration and the sum of the signal intensity of all "positive contrast voxels" within a region-of-interest at the spot location. A voxel was considered "positive contrast" if its signal intensity was >3 times the standard deviation above the background signal level. The two methods showed different slopes for the signal dependence on concentration highlighting their different sensitivities. Though the off-resonance method had higher integrated signal intensity for the 75 μg/ml voxel, the SGM map provided a higher contrast-to-noise ratio (CNR) than the off-resonance image, as the number of "positive contrast voxels" in the off-resonance image was greater. For the images in Fig. 1 the CNR ranged between 4.8-13.6 for the four magnetite spots in the off-resonance image and between 26.6-31.8 in the SGM map.

With the potential to quantify their contrast enhancement, positive contrast MRI of magnetotactic bacteria can be a useful tool for studying cancer diagnosis and treatment evaluation in pre-clinical models. The bacteria naturally generate magnetite particles providing an endogenous contrast source, which could overcome the problem of dilution when using exogenously introduced particles.

Future work will involve further investigating the sensitivity of the two methods and the minimum detection limit of Fe concentration for both techniques and applying these in an in vivo tumor model.

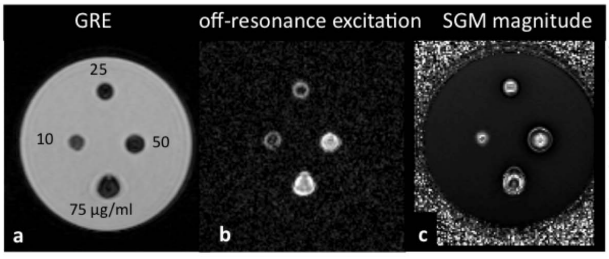

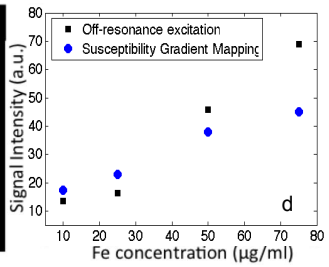

References: [1] Benoit et al [2009] Clin Cancer Res 15:5170-5177
[2] Cunningham et al [2005], MRM 53:999-1005 [3] Dahnke et al [2008] MRM 60:595-603

Acknowledgements: R21 CA140903
P41 RR009784, P50 CA114747